J|A|C|S
ARTICLES
Published on Web 10/19/2004

On the Competition between Linear and Cyclic Isomers in Second-Row Dicarbides

Antonio Largo,* Pilar Redondo, and Carmen Barrientos

Contribution from the Departamento de Química Física, Facultad de Ciencias, Universidad de Valladolid, 47005 Valladolid, Spain

Received July 5, 2004; E-mail: alargo@qf.uva.es

Abstract: Second-row dicarbides C_2X (X = Na−Cl) are investigated with quantum mechanical techniques. The cyclic−linear competition in these systems is studied, and the bonding scheme for these compounds is discussed in terms of the topological analysis of the electronic density. C_2Na, C_2Mg, C_2Al, and C_2Si are found to prefer a C_{2v}-symmetric arrangement corresponding to a T-shape structure. On the other hand, for C_2P, C_2S, and C_2Cl the linear isomer is predicted to be the ground state. A detailed analysis of the variation of the electronic energy and orbital energies with the geometry has been carried out. A simple theoretical model, taking into account the main interactions between the valence orbitals of both fragments, the X atom and the C_2 molecule, allows an interpretation of the main features of these compounds.

Introduction

C_2X compounds containing second-row atoms (X = Na−Cl) are molecules of interest in astrochemistry. In fact, some of them have already been detected in space, such as C_2Si[1−4] and C_2S,[5−8] and it is thought that quite likely other members of the same family could be eventually detected in interstellar clouds or circumstellar envelopes.

A milestone in the study of C_2X compounds was undoubtedly the discovery of the structure of C_2Si in 1984. In that year, Grev and Schaefer[9] and Smalley et al.[10] conducted parallel theoretical and experimental, respectively, investigations on silicon dicarbide. The theoretical study predicted that the lowest-lying isomer of silicon dicarbide is a ring structure, with the linear SiCC structure lying about 5 kcal/mol higher in energy. This cyclic ground state was confirmed by the experiment,[10] and immediately the radioastronomical detection of silicon dicarbide was possible[1]. Since then many experimental studies on silicon dicarbide have been carried out.[11−18] From the theoretical side a number of studies on C_2Si has also appeared in recent years,[19−26] most of them dealing with the energy difference between the linear and cyclic arrangements at different levels of theory. The theoretical studies confirmed the prediction of Grev and Schaefer,[9] thus obtaining a C_{2v}-symmetric ground state. However, it is also shown in these works that the potential surface for the cyclic-linear interconversion is rather flat, and therefore that the system behaves as a molecular pinwheel. Also, as discussed by Nielsen et al.,[23] the theoretical description of C_2Si has remained as a challenge to ab initio methods, because it requires both large basis sets and high-order correlation treatments for an accurate description.

Following the interest on C_2Si, other second-row dicarbides were theoretically studied. C_2S, mainly because of its interstellar relevance, has also been the subject of different theoretical works.[27−29] Much effort has been devoted to the theoretical prediction of structural properties of other dicarbides in order to aid in their possible identification in astronomical sources.

(1) Thaddeus, P.; Cummins, S. E.; Linke, R. A. *Astrophys. J. Lett.* **1984**, *283*, L25.
(2) Snyder, L. E.; Henkel, C.; Hollis, J. M.; Lovas, F. J. *Astrophys. J.* **1985**, *290*, L29.
(3) Cernicharo, J.; Kahane, C.; Gomez-Gonzalez, J.; Guelin, M. *Astron. Astrophys.* **1986**, *167*, L9.
(4) Cernicharo, J.; Guélin, M.; Kahane, C. *Astron. Astrophys. Suppl.* **2000**, *142*, 181.
(5) Cernicharo, J.; Guélin, M.; Hein, H.; Kahane, C. *Astron. Astrophys.* **1987**, *181*, L9.
(6) Saito, S.; Kawaguchi, K.; Yamamoto, S.; Ohishi, M.; Suzuki H.; Kaifu, N. *Astrophys. J.* **1987**, *317*, L115.
(7) Cernicharo, J.; Gottlieb, C. A.; Guelin, M.; Thadeus, P.; Vrtilek, J. M. *Astrophys. J. Lett.* **1989**, 341 L25.
(8) Fuente, A.; Cernicharo, J.; Barcia, A.; Gomez-Gonzalez, J. *Astron. Astrophys.* **1990**, *231*, 151.
(9) Grev, R. S.; Schaefer, H. F. *J. Chem. Phys.* **1984**, *80*, 3552.
(10) Michalopoulos, D. L.; Geusic, M. E.; Langridge-Smith, P. R. R.; Smalley, R. E. *J. Chem. Phys.* **1984**, *80*, 3556.
(11) Shepherd, R. A.; Graham, W. R. M. *J. Chem. Phys*. **1985**, *82*, 4788.
(12) Presilla-Marquez, J. D.; Graham, W. R. M.; Shepherd, R. A. *J. Chem. Phys.* **1990**, *93*, 5424.
(13) Bredohl, H.; Dubois, I.; Leclercq, H.; Melen, F. *J. Mol. Spectrosc*. **1988**, 128, 399.
(14) Suenram, R. D.; Lovas, F. J.; Matsumura, K. *Astrophys. J.* **1989**, *342*, L103
(15) Gottlieb, C. A.; Vrtilek, J. M.; Thaddeus, P. *Astrophys. J.* **1989**, *343*, L29.
(16) Cernicharo, J.; Guelin, M.; Kahane, C.; Bogey, M.; Demuynck, C.; Destombes, J. L. *Astron. Astrophys.* **1991**, *246*, 213.
(17) Izuha, M.; Yamamoto, S.; Saito, S. *Spectrochim. Acta A* **1994**, *50*, 1371.
(18) Ross, S. C.; Butenhoff, T. J.; Rohlfing, E. A.; Rohlfing, C. M. *J. Chem. Phys.* **1994**, *100*, 4110.
(19) Oddershede, J.; Sabin, J. R.; Diercksen, G. H. F.; Grüner, N. E. *J. Chem. Phys*. **1985**, *83*, 1702.
(20) Fitzgerald, G.; Cole, S. J.; Bartlett, R. J. *J. Chem. Phys.* **1986**, *85*, 1701.
(21) Sadlej, A. J.; Diercksen, G. H. F.; Oddershede, J.; Sabin, J. R. *Chem. Phys.* **1988**, *122*, 297.
(22) Deutsch, P. W.; Curtiss, L. A. *Chem. Phys. Lett.* **1994**, *226*, 387.
(23) Nielsen, I. M. B.; Allen, W. D.; Csaszar, A. G.; Schaefer, H. F. *J. Chem. Phys.* **1997**, *107*, 1195.
(24) Zhang, Y.; Zhao, C.; Fang, W.; Lu, Z. *J. Mol. Struct. (THEOCHEM)* **1998**, *454*, 31.
(25) Arulmozhiraja, S.; Kolandaivel, P.; Ohashi, O. *J. Phys. Chem. A* **1999**, *103*, 3073.
(26) Kenny, J. P.; Allen, W. D.; Schaefer, H. F. *J. Chem. Phys.* **2003**, *118*, 7353.
(27) Murakami, A. *Astrophys. J.* **1990**, *357*, 288.
(28) Peeso, D. J.; Ewing, D. W.; Curtis, T. T. *Chem. Phys. Lett*. **1990**, *166*, 307.
(29) Xie, Y.; Schaefer, H. F. *J. Chem. Phys.* **1992**, *96*, 3714.

Theoretical predictions for C_2Mg,[30−32] C_2Al,[33−39] C_2P,[40,41] and C_2Cl[42−44] have also appeared.

There is another reason for the relevance of second-row atom dicarbides. Carbon clusters mixed with heteroatoms have attracted a growing interest in recent years because of their interest for new materials science, and this has stimulated different studies on C_nX compounds. Since small heteroatom-doped carbides, such as C_2X, are the basic structural units for these clusters, it is of utmost importance to have a detailed knowledge of the structure and properties of C_2X molecules. Much of the interest has focused on nonmetallic elements, and therefore different theoretical works have studied the neutral and charged C_nS,[45−48] C_nSi,[49−51] C_nP,[52−54] and C_nCl[55] clusters. In addition heteroatom-doped carbon clusters containing metallic elements, such as C_nAl,[56] C_nMg,[57,58] and C_nNa[59] have also been studied in last years. All these works tried to identify systematic trends on the properties of these compounds as a function of the cluster size. Of particular relevance is a comprehensive analysis of the properties of linear carbon clusters doped with second-row elements by Li and Tang.[60] Laboratory detections of second-row heteroatom-doped carbon clusters have also been reported,[61] as well as experiments concerning charged species.[62,63] We should also recall that C_2X compounds are also relevant as building blocks for metal carbides and metallocarbohedrenes (metcars), a subject that has attracted considerable attention in recent years.[64−68]

A key feature of C_2X compounds containing second-row atoms is the competition between linear and cyclic arrangements, and even the nature of the apparently cyclic isomer, because the C_{2v}-symmetric species could be in fact best described as a T-shape structure. The main purpose of the present paper is to analyze in detail the factors governing this competition between linear and cyclic species for C_2X (X = Na−Cl) molecules, trying to rationalize the structure of these compounds.

Theoretical Methods

Although we have carried out computations at several levels of theory we will only report those that we consider more representative. We have employed two different theoretical approaches in order to obtain the geometrical parameters of C_2X compounds. One of the levels employed corresponds to the density functional theory (DFT) formalism, which has proved in recent years to be a relatively low-cost approach with a reasonable performance. In particular, we have used one of the most popular DFT methods, namely the B3LYP approach, which is extensively employed in chemical computations. The B3LYP level consists of the Lee−Yang−Parr[69] correlation functional in conjunction with a hybrid exchange functional first proposed by Becke.[70] In addition, we have also employed the so-called QCISD method[71] (quadratic configuration interaction including single and double excitations), which is considered to be one of the most reliable ab initio methods for predicting geometrical parameters. In both cases, the 6-311+G(3df) basis set[72] was employed, thus including three sets of d polarization functions, one set of f polarization functions, and diffuse functions as well. We chose this basis set because it has been shown that in certain C_2X compounds, such as C_2Si,[23] a good theoretical level is required for a proper description. Harmonic vibrational frequencies were also computed at both levels, B3LYP and QCISD, with the 6-311+G(3df) basis set. These calculations allow not only an estimate of the zero-point vibrational energy (ZPVE), but also to assess the nature of the stationary points and therefore characterize if they are true minima on the respective potential surface. To improve the computation of relative energies we have carried out single-point calculations on the QCISD geometries with the CCSD(T) approach[73] (coupled-cluster single and double excitation model augmented with a noniterative treatment of triple excitations) with the 6-311+G(3df) basis set. All these calculations were carried out with the Gaussian 98 program package.[74]

The nature of bonding for the different C_2X species was characterized through the topological analysis of the electronic density.[75] These calculations were performed with the MORPHY program,[76] employing the QCISD/6-311+G(d) electronic density. An analysis in terms of natural bond orbitals (NBO)[77] has also been carried out.

(30) Green, S. *Chem. Phys. Lett.* **1984**, *112*, 29.
(31) Woon, D. E. *Astrophys. J.* **1996**, *456*, 602.
(32) Boldyrev, A. I.; Simons, J. *J. Phys. Chem. A* **1997**, *101*, 2215.
(33) Flores, J. R.; Largo, A. *Chem. Phys.* **1990**, *140*, 19.
(34) Knight, L. B.; Cobranchi, S. T.; Herlong, J. O.; Arrington, C. A. *J. Chem. Phys.* **1990**, *92*, 5856.
(35) Chertihin, G. V.; Andrews, L.; Taylor, P. R. *J. Am. Chem. Soc.* **1994**, *116*, 3513.
(36) Ma, B.; Yamaguchi, Y.; Schaefer, H. F. *Mol. Phys.* **1995**, *86*, 1331.
(37) Yang, H. L.; Tanaka, K.; Ahinada, M. *J. Mol. Struct. (THEOCHEM)* **1998**, *422*, 159.
(38) Lanzisera, D. V.; Andrews, L. *J. Phys. Chem. A* **1997**, *101*, 9660.
(39) Boldyrev, A.; Simons, J.; Li, X.; Wang, L. S. *J. Am. Chem. Soc.* **1999**, *121*, 10193.
(40) Largo, A.; Barrientos, C.; Lopez, X.; Ugalde, J. M. *J. Phys. Chem*. **1994**, *98*, 3985.
(41) El-Yazal, J.; Martin, J. M. L.; Francois, J. P. *J. Phys. Chem. A* **1997**, *101*, 8319.
(42) Largo-Cabrerizo, A.; Barrientos, C. *Chem. Phys. Lett.* **1989**, *155*, 550.
(43) Largo, A.; Barrientos, C. *Chem. Phys.* **1989**, *138*, 291.
(44) Sumiyoshi, Y.; Ueno, T.; Endo, Y. *J. Chem. Phys.* **2003**, *119*, 1426.
(45) Lee, S. *Chem. Phys. Lett.* **1997**, *268*, 69.
(46) Pascoli, G.; Lavendy, H. *Int. J. Mass Spectrom.* **1998**, *181*, 11.
(47) Pascoli, G.; Lavendy, H. *Int. J. Mass Spectrom.* **1998**, *181*, 135.
(48) Tang, Z.; BelBruno, J. J. *Int. J. Mass Spectrom.* **2001**, *208*, 7.
(49) Fye, J. L.; Jarrold, M. F. *J. Phys. Chem. A* **1997**, *101*, 1836.
(50) Pascoli, G.; Lavendy, H. *Int. J. Mass Spectrom. Ion Proc.* **1998**, *173*, 41.
(51) Pascoli, G.; Lavendy, H. *Int. J. Mass Spectrom. Ion Proc.* **1998**, *177*, 31.
(52) Zhan, C.; Iwata, S. *J. Chem. Phys.* **1997**, *107*, 7323.
(53) Pascoli G.; Lavendy H. *J. Phys. Chem. A* **1999**, *103*, 3518.
(54) Pascoli, G.; Lavendy, H. *Int. J. Mass Spectrom.* **1999**, *189*, 125.
(55) Largo, A.; Cimas, A.; Redondo, P.; Barrientos, C. *Int. J. Quantum Chem.* **2001**, *84*, 127.
(56) Largo, A.; Redondo, P.; Barrientos, C. *J. Phys. Chem. A* **2002**, *106*, 4217.
(57) Redondo, P.; Barrientos, C.; Cimas, A.; Largo, A. *J. Phys. Chem. A* **2003**, *107*, 4676.
(58) Redondo, P.; Barrientos, C.; Cimas, A.; Largo, A. *J. Phys. Chem. A* **2003**, *107*, 6317.
(59) Redondo, P.; Barrientos, C.; Cimas, A.; Largo, A. *J. Phys. Chem. A* **2004**, *108*, 212.
(60) Li, G.; Tang, Z. *J. Phys. Chem. A* **2003**, *107*, 5317.
(61) McCarthy, M. C.; Apponi, A. J.; Gottlieb, C. A.; Thadeus, P. *Astrophys. J.* **2000**, *538*, 766.
(62) Nakajima, A.; Taguwa, T.; Nakao, K.; Gomei, M.; Kishi, R.; Iwata, S.; Kaya, K. *J. Chem. Phys.* **1995**, *103*, 2050.
(63) Liu, Z.; Huang, R.; Tang, Z.; Zheng, L. *Chem. Phys.* **1998**, *229*, 335.
(64) Li, S.; Hongbin, W.; Wang, L. S. *J. Am. Chem. Soc.* **1997**, *119*, 7417.
(65) Rohmer, M. M.; Benard, M.; Poblet, J. M. *Chem. Rev.* **2000**, *100*, 495.
(66) Liu, P.; Rodriguez, J. A.; Hou, H.; Muckerman, J. T. *J. Chem. Phys.* **2003**, *118*, 7737.
(67) Liu, P.; Rodriguez, J. A. *J. Chem. Phys.* **2004**, *120*, 5414.
(68) Gueorguiev, G. K.; Pacheco, J. M. *Phys. Rev. Lett.* **2002**, *88*, 115504.
(69) Lee, C.; Yang, W.; Parr, R. G. *Phys. Rev. B* **1988**, *37*, 785.
(70) Becke, A. D. *J. Chem. Phys.* **1988**, *88*, 1053.
(71) Pople, J. A.; Head-Gordon, M.; Raghavachari, K. *J. Chem. Phys.* **1987**, *87*, 5968.
(72) Hehre, W. J.; Radom, L.; Schleyer, P. v. R.; Pople, J, A. *Ab Initio Molecular Orbital Theory*; Wiley: New York, 1986.
(73) Raghavachari, K.; Trucks, G. W.; Pople, J. A.; Head-Gordon, M. *Chem. Phys. Lett.* **1989**, *157*, 479.
(74) Frisch, M. J.; Trucks, G. W.; Schlegel, H. B.; Scuseria, G. E.; Robb, M. A.; Cheeseman, J. R.; Zakrzewski, V. G.; Montgomery. J. A., Jr.; Stratmann, R. E.; Burant, J. C.; Dapprich, S.; Millan, J. M.; Daniels, A. D.; Kudin, K. N.; Strain, M. C.;. Farkas, O.; Tomasi, J.; Barone, V.; Cossi, M.; Cammi, R.; Mennucci, B.; Pomelly, C.; Adamo, C.; Clifford, S.; Ochterski, J.; Petersson, G. A.; Ayala, P. Y.; Cui, Q.; Morokuma, K.; Malick, D. K.; Rabuck, A. D.; Raghavachari, K.; Foresman, J. B.; Cioslowski, J.; Ortiz, J. V.; Baboul, A. G.; Stefanov, B. B.; Liu, G.; Liashenko, A.; Piskorz, P.; Komaromi, I.; Gomperts, R.; Martin, R. L.; Fox, D. J.; Keith, T.; Al-Laham, M. A.; Peng, C. Y.; Nanayakkara, A.; Gonzalez, C.; Challacombe, M.; Gill, P. M. W.; Johnson, B.; Chen, W.; Wong, M. W.; Andres, J. L.; Gonzalez, C.; Head-Gordon, M.; Replogle, E. S.; Pople, J. A. Gaussian 98; Gaussian Inc: Pittsburgh, PA, 1998.
(75) Bader, R. F. W. *Atoms in Molecules. A Quantum Theory*; Clarendon Press: Oxford, 1990.
(76) Popelier, P. L. A. *Comput. Phys. Commun*. **1996**, *93*, 212.
(77) Reed, A. E.; Curtiss, L. A.; Weinhold, F. *Chem. Rev.* **1988**, *88*, 899.

Table 1. Electronic Configurations, Geometrical Parameters, and Harmonic Vibrational Frequencies for Linear C_2X Species Obtained with the B3LYP/6-311+G(3df) and QCISD/6-311+G(3df) (second line) Methods

linear C_2X	electronic configuration	linear geometry (Å) R(X–C)	linear geometry (Å) R(C–C)	vibrational frequencies (cm^{-1})
C_2Na ($^2\Sigma$)	{core}$6\sigma^2 7\sigma^2 2\pi^4 8\sigma^1$	2.214	1.238	188i(π), 381(σ), 1948(σ)
		2.249	1.246	90i(π), 371(σ), 1943(σ)
C_2Mg ($^1\Sigma$)	{core}$6\sigma^2 7\sigma^2 2\pi^4 8\sigma^2$	1.938	1.251	76(π), 556(σ), 1918(σ)
		1.995	1.234	171i(π), 587(σ), 1944(σ)
C_2Al ($^2\Sigma$)	{core}$6\sigma^2 7\sigma^2 8\sigma^2 2\pi^4 9\sigma^1$	1.878	1.245	75(π), 511(σ), 1850(σ)
		1.828	1.259	102i(π), 578(σ), 1805(σ)
C_2Si ($^1\Sigma$)	{core}$6\sigma^2 7\sigma^2 8\sigma^2 2\pi^4 9\sigma^2$	1.693	1.276	23i(π), 797(σ), 1928(σ)
		1.687	1.281	74i(π), 816(σ), 1925(σ)
C_2P ($^2\Pi$)	{core}$6\sigma^2 7\sigma^2 8\sigma^2 2\pi^4 9\sigma^2 3\pi^1$	1.606	1.301	162(π), 275(π), 852(σ), 1726(σ)
		1.604	1.311	231(π), 279(π), 850(σ), 1694(σ)
C_2S ($^3\Sigma$)	{core}$6\sigma^2 7\sigma^2 8\sigma^2 2\pi^4 9\sigma^2 3\pi^2$	1.566	1.308	287(π), 868(σ), 1727(σ)
		1.564	1.315	298(π), 879(σ), 1746(σ)
C_2Cl ($^2\Pi$)	{core}$6\sigma^2 7\sigma^2 8\sigma^2 2\pi^4 9\sigma^2 3\pi^3$	1.615	1.283	334i(π), 297(π), 742(σ), 1890(σ)
		1.620	1.289	292(π), 719(π), 751(σ), 1904(σ)

Table 2. Electronic Configurations, Geometrical Parameters, and Harmonic Vibrational Frequencies for Cyclic C_2X Species Obtained with the B3LYP/6-311+G(3df) and QCISD/6-311+G(3df) (second line) Methods

cyclic C_2X	electronic configuration	cyclic geometry (Å,degrees) R(X–C)	cyclic geometry (Å,degrees) R(C–C)	cyclic geometry (Å,degrees) ∠CXC	vibrational frequencies (cm^{-1})
C_2Na ($^2A_1$)	{core}$5a_1^2 6a_1^2 3b_2^2 2b_1^2 7a_1^1$	2.359	1.260	31.0	225(b_2), 371(a_1), 1831(a_1)
		2.390	1.276	30.9	224(b_2), 360(a_1), 1769(a_1)
C_2Mg ($^1A_1$)	{core}$5a_1^2 3b_2^2 6a_1^2 2b_1^2 7a_1^2$	2.013	1.265	36.6	417(b_2), 613(a_1), 1773(a_1)
		2.040	1.271	36.3	417(b_2), 538(a_1), 1781(a_1)
C_2Al ($^2A_1$)	{core}$5a_1^2 6a_1^2 3b_2^2 2b_1^2 7a_1^2 8a_1^1$	1.932	1.261	38.3	373(b_2), 625(a_1), 1802(a_1)
		1.922	1.272	38.7	419(b_2), 652(a_1), 1773(a_1)
C_2Si ($^1A_1$)	{core}$5a_1^2 6a_1^2 3b_2^2 2b_1^2 7a_1^2 8a_1^2$	1.844	1.260	40.0	123(b_2), 794(a_1), 1838(a_1)
		1.836	1.270	40.5	153(b_2), 822(a_1), 1806(a_1)
C_2P ($^2B_2$)	{core}$5a_1^2 6a_1^2 3b_2^2 2b_1^2 7a_1^2 8a_1^2 4b_2^1$	1.749	1.327	44.6	390(b_2), 794(a_1), 1510(a_1)
		1.748	1.336	44.9	244(b_2), 802(a_1), 1497(a_1)
C_2S ($^3A_2$)	{core}$5a_1^2 6a_1^2 3b_2^2 2b_1^2 7a_1^2 8a_1^2 4b_2^1 3b_1^1$	1.780	1.297	42.7	616i(b_2), 729(a_1), 1644(a_1)
		1.775	1.308	43.3	55(b_2), 746(a_1), 1614(a_1)
C_2Cl ($^2B_1$)	{core}$5a_1^2 6a_1^2 3b_2^2 7a_1^2 2b_1^2 4b_2^2 8a_1^2 3b_1^1$	1.901	1.364	42.0	267(b_2), 564(a_1), 1404(a_1)
		1.893	1.372	42.5	287(b_2), 577(a_1), 1418(a_1)

Results and Discussion

Overview of the Molecular Structure of C_2X Compounds. We have carried out calculations for the lowest-lying linear and C_{2v}-symmetric C_2X species (the $D_{\infty h}$ isomers with C−X−C connectivity lie in all cases much higher in energy). In most cases the electronic states correspond to low spin states (singlet for closed-shells, doublet for open-shells). There is only one exception, namely C_2S, which is known to have a linear triplet ground state.[27−29] Consequently, we will report the results for the linear $^3\Sigma$ state and the corresponding lowest-lying cyclic triplet state ($^3A_2$). Nevertheless, we have also considered the lowest-lying singlet states (linear and cyclic) of C_2S, and we will also refer to their results when needed. The case of C_2Cl deserves also some comments. A recent combined experimental and ab initio study[44] suggests that this should be a bent molecule, with a bond angle near 157°, although the linear structure should lie very close in energy (less than 500 cm^{-1} above the bent species) according to the theoretical calculations. Furthermore, in the linear limit there are two different electronic states, $^2\Sigma$ and $^2\Pi$ lying very close in energy. The recent multireference study[44] predicts that the $^2\Sigma$ state should lie lower in energy (about 200 cm^{-1}), whereas previous studies[42,43] placed the $^2\Pi$ state about 400 cm^{-1} below the $^2\Sigma$ one. We have adopted the $^2\Pi$ electronic state in linear geometries because at the levels of theory employed in the present work it is found to lie below the $^2\Sigma$ state by 1585, 165, and 164 cm^{-1} at the B3LYP, QCISD, and CCSD(T) levels, respectively. In any case, the conclusions should be very similar employing any of these states, given their proximity in energy. Furthermore, the lowest-lying cyclic state ($^2B_1$) correlates with the $^2\Pi$ state.

The geometrical parameters and vibrational frequencies for the linear isomers of the different C_2X species are given in Table 1, whereas in Table 2 the corresponding data for the C_{2v}-symmetric structures are shown. There is an overall reasonable agreement between the B3LYP and QCISD geometrical parameters, with mean deviations between both levels of theory for the X−C and C−C distances of 0.018 Å and 0.010 Å, respectively. As expected the X−C distance in the linear species decreases as one moves toward the right side of the periodic table, with the only exception of C_2Cl, where it is increased with respect to its sulfur counterpart. The same is true for the cyclic isomers, but in this case the inversion in the trend occurs for C_2S. The C−C distances for the linear isomers are all intermediate between those of typical double and triple bonds, and are shorter for Na, Mg, Al, and Si compounds than for P, S, and Cl species. The same is true for the cyclic isomers. In fact, for Na−Si dicarbides the C−C bond distances are quite close to the bond length in C_2, namely 1.247 Å and 1.250 Å, respectively, at the B3LYP and QCISD levels with the 6-311+G(3df) basis set.

Concerning the vibrational frequencies there are some important qualitative differences between the B3LYP and QCISD levels. Whereas for linear C_2Na and C_2Si both levels provide imaginary frequencies associated to the bending modes,

Table 3. Relative Energies ($E_{cyclic}-E_{linear}$) (kcal/mol), for Cyclic C_2X Species at Different Levels of Theory Including ZPVE Corrections[a]

	level				ΔE_{corr}(l–c)
C_2X	HF	B3LYP	QCISD	CCSD(T)	CCSD(T)
C_2Na	−4.01	−9.05	−10.28	−9.44	5.49
C_2Mg	−26.31	−15.90	−12.87	−12.03	−13.98
C_2Al	−17.71	−9.35	−16.90	−14.98	−2.07
C_2Si	−0.38	0.20	−4.81	−3.80	3.48
C_2P	11.38	6.32	4.28	3.37	7.50
$C_2S(1)$[b]	9.22	9.64	6.77	5.74	2.82
$C_2S(3)$[c]	44.94	35.89	33.68	31.50	12.29
C_2Cl	35.14	32.29	31.30	30.32	2.84

[a] In the case of CCSD(T) calculations, QCISD ZPVE values have been employed. The difference between the correlation energies (in kcal/mol), computed at the CCSD(T) level, for linear and cyclic isomers is also given in the last column. [b] Singlet state. [c] Triplet state.

in the cases of C_2Mg and C_2Al the B3LYP level produces real π frequencies, thus predicting that these linear species are true minima. In these last two cases, when we tried to follow the bending mode and optimize a possible C_s structure at the QCISD level all our attempts failed, and therefore, there seems that there is not a bent minimum for these dicarbides. A different behavior is observed for the other linear species where there is a discrepancy in the vibrational frequencies at the B3LYP and QCISD levels, namely C_2Cl. In this case, it is possible to obtain a bent minimum at both levels of theory which lies slightly below the corresponding linear species (about 0.7 and 3.2 kcal/mol at the B3LYP and QCISD levels, respectively), despite at the QCISD level the latter has all its frequencies real. The bond angle for the bent structure is close to that found in a recent theoretical study,[44] namely 165.3° and 169.6°, respectively, at the B3LYP and QCISD levels of theory. Therefore, it seems that this is the only case where a bent ground state is predicted, in agreement with the previous study at different levels of theory.[44] For the cyclic isomers, there is only one discrepancy in the vibrational frequencies. At the B3LYP level, cyclic C_2S ($^3A_2$ electronic state) has an imaginary frequency, whereas at the QCISD level it is predicted to be a true minimum, although it has a very low b_2 frequency (55 cm^{-1}). For the rest of cyclic species, the agreement in the vibrational frequencies computed at both levels is reasonably good.

The energy differences between cyclic and linear species at the three levels of theory employed in the present work, including ZPVE corrections, are given in Table 3. There is in general a reasonable agreement between the QCISD and CCSD(T) values, with discrepancies of about 2 kcal/mol in the worst cases. In fact, the rather affordable B3LYP method performs not too badly. Although the largest discrepancy with CCSD(T) values is about 5 kcal/mol, the B3LYP results predict the correct energy ordering with the only exception of C_2Si, which is recognized to be a difficult case.[18−26] From the results shown in Table 3, and taken into account the previous theoretical studies carried out for most of these systems, it seems quite safe to conclude that metal dicarbides have C_{2v}-symmetric ground states, whereas nonmetal dicarbides have linear (or slightly bent, as in the case of C_2Cl) ground states. C_2Si is at the borderline between both behaviors, with linear and C_{2v}-symmetric species lying very close in energy, although the higher levels of theory confirm that it behaves as the metal dicarbides.

Another interesting feature is the type of interaction that takes place between the heteroatom and the carbon atoms in C_2X compounds. To characterize this interaction, as well as to establish what is the bonding scheme in these dicarbides, we have carried out a topological analysis of the electronic density in terms of Bader's theory.[75] This analysis allows to characterize the chemical nature of the bonding. Extrema or critical points in the one-electron density $\rho(r)$ computed at the QCISD/6-311+G(d) level were identified. In our case, only *bond critical points*[75] (corresponding to a minimum value of $\rho(r)$ along the line linking the nuclei and a maximum along the interatomic surfaces) and *ring critical points*[75] ($\rho(r)$ being a minimum in two directions and a maximum in one direction) are relevant. We will only focus on a few important properties of critical points which are the most relevant for our purposes, namely the electronic density $\rho(r)$ at the critical point, the Laplacian of the charge density $\nabla^2\rho(r)$, and the total energy density $H(r)$. The chemical nature of the bonding can be determined according to the values of the charge density and its Laplacian at the bond critical point. There are basically two limiting types of atomic interactions, namely shared and closed-shell interactions.[75] Of course, there is a whole spectrum of intermediate interactions lying between the two extreme cases.[78]

Shared interactions are in general characterized by large electronic densities and negative values of the Laplacian,[75] and are characteristic of covalent compounds. On the other hand, closed-shell interactions correspond to relatively low $\rho(r)$ and positive values of $\nabla^2\rho(r)$,[75] a situation which is usually found for ionic and van der Waals compounds. Nevertheless in some cases, to characterize the covalency degree of a bond, the total energy density, $H(r)$, which is the sum of the potential and kinetic energy density at a critical point, might be useful. If $H(r) < 0$ the system is stabilized by accumulation of electronic charge in the internuclear region, showing the characteristics of a covalent interaction.[75] Conversely, if $H(r)$ is positive, accumulation of electronic charge would lead to a destabilization of the system, a typical feature of van der Waals and ionic bonding systems.

In Table 4 we provide the $\rho(r)$, $\nabla^2\rho(r)$, and $H(r)$ values at the bond critical points obtained with the QCISD/6-311+G(d) electronic density. First it should be noted that in the case of the C_{2v}-symmetric isomers of C_2Na, C_2Mg, C_2Al, and C_2Si there is no ring critical point, and, together with the C−C bond critical point, only a bond critical point between the heteroatom and the middle point of the C_2 unit was found. Therefore these species are in fact T-shape compounds rather than truly cyclic molecules. On the other hand, for the nonmetal dicarbides C_2P, C_2S, and C_2Cl the topological analysis of the electronic density of the C_{2v}-symmetric species allows to characterize two individual X−C bond critical points, along with a ring critical point. These features evidence that these compounds are truly cyclic species. Nevertheless, we must point out that for cyclic C_2P the two P−C bond critical points are rather curved and are located relatively close (and with $\rho(r)$ values very close to that of the ring critical point), indicating that this species is not far from a T-shape description.

From the data shown in Table 4 it can be concluded that the Na, Mg, and Al linear dicarbides exhibit mainly ionic X−C bonds, since they are characterized by low values of $\rho(r)$, always

(78) Bader, R. F. W. *Chem. Rev.* **1991**, *91*, 893.

Table 4. Summary of Critical Point Data for the Linear and Cyclic Isomers of C_2X Species, Using the QCISD/6-311+G(d) Electronic Density

isomer	type		Na	Mg	Al	Si	P	S	Cl
linear	X−C bond	$\rho(r)$	0.03199	0.05860	0.09134	0.14618	0.19514	0.24798	0.25018
		$\nabla^2\rho(r)$	0.17623	0.35512	0.45253	0.64993	0.64959	0.29964	−0.48829
		$-H(r)$	0.03969	0.08679	0.13664	0.24574	0.33541	0.38688	0.10636
	C−C bond	$\rho(r)$	0.34775	0.38189	0.36486	0.38210	0.35881	0.34533	0.34728
		$\nabla^2\rho(r)$	−0.90098	−1.16399	−1.09206	−1.3115	−1.20394	−1.14156	−1.07232
		$-H(r)$	0.25833	0.27386	0.21290	0.17513	0.15536	0.17938	0.23396
cyclic	X−C_2 bond	$\rho(r)$	0.02466	0.05399	0.08056	0.11656			
		$\nabla^2\rho(r)$	0.14006	0.35605	0.43913	0.42333			
		$-H(r)$	0.02977	0.08418	0.12567	0.17108			
	X−C bond	$\rho(r)$					0.16192	0.17772	0.13803
		$\nabla^2\rho(r)$					0.24926	0.01311	0.18465
		$-H(r)$					0.21352	0.12295	0.10716
	C−C bond	$\rho(r)$	0.34235	0.36727	0.38247	0.40064	0.35832	0.38044	0.35180
		$\nabla^2\rho(r)$	−0.91664	−1.07126	−1.18807	−1.33783	−1.09669	−1.25260	−1.15070
		$-H(r)$	0.21110	0.21867	0.21716	0.21676	0.17059	0.18295	0.13065

Table 5. NBO Atomic Charges at the B3LYP/6-311+G(3df) Level

isomer	atomic charge	Na	Mg	Al	Si	P	S	Cl
linear	Q(X)	0.935	1.223	1.006	1.109	0.750	0.414	0.248
	$Q(C_1)$	−0.859	−1.188	−1.165	−1.300	−0.942	−0.517	−0.264
	$Q(C_2)$	−0.076	−0.045	0.159	0.191	0.192	0.103	0.016
cyclic	Q(X)	0.918	1.282	1.086	1.002	0.754	0.470	0.150
	Q(C)	−0.459	−0.641	−0.543	−0.501	−0.377	−0.235	−0.075

lower than 0.1 au, and positive values of the Laplacian (compared with the corresponding values of C−C bond critical points, typical of a covalent interaction). Nevertheless, the negative (although low) value of $H(r)$ suggests a small degree of covalency. On the other hand for linear C_2Cl all parameters (relatively large $\rho(r)$ and a negative Laplacian) are compatible with a standard covalent interaction. Finally for the Si, P, and S linear dicarbides the critical points data (relatively large $\rho(r)$ and a positive value of $\nabla^2\rho(r)$) suggest intermediate interactions. For the C_{2v}-symmetric species a similar behavior is generally observed, except in two cases. The most evident case is C_2Cl, where now the Laplacian for the X−C bond critical point is positive and it seems more appropriate to classify the interaction in this case as an intermediate one. The much lower value of $\rho(r)$ found in the cyclic isomer (0.13803 au) compared with the linear one (0.25018 au) points also in the same direction. More subtle are the changes observed for T-shape C_2Si when compared with the linear species. For the T-shape isomer the electronic density is lower (0.11656 au, compared with the value of 0.14618 au for the linear isomer), and not much different from the value observed for C_2Al (0.08056 au), which suggests that quite likely the interaction could be more properly classified as a ionic one.

Another clue for analyzing the ionic nature of the bonding in C_2X compounds is provided by the net atomic charges, even though these values should be taken with caution and only as tentative indicators. In Table 5 we have collected the atomic charges of the different linear and cyclic C_2X species obtained through a Natural Bond Orbital (NBO)[77] analysis at the B3LYP/6-311+G(3df) level. It is clearly seen in Table 5 that for both linear and cyclic species containing Na, Mg, Al, and Si the net charge at the heteroatom is nearly +1e. In other words one can see that there is net transfer of one electron from X toward the C_2 unit. For the P, S, and Cl compounds it is observed as expected that the net charge at X decreases monotonically.

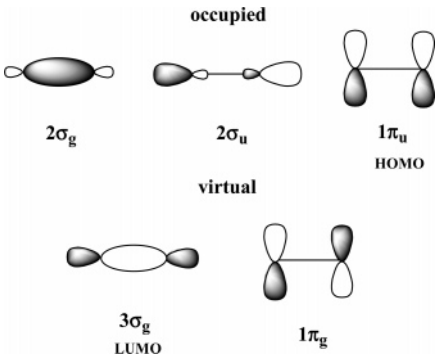

Figure 1. Schematic representation of the molecular orbitals for the C_2 molecule.

A Theoretical Model. It would be desirable to have a simple bonding model that could describe the C_2X compounds. For example, the model developed by Dewar[79] and by Chatt and Duncanson,[80] originally devised for metal-olefin systems, also provides a reasonable explanation for the interaction of transition metals and strained rings, and has been applied in different three-membered ring systems.[81−86] An approximation to a theoretical model for C_2X compounds can be developed bearing in mind the form of the molecular orbitals of the C_2 unit, which are schematically depicted in Figure 1. The main relevant interactions between these orbitals and the corresponding valence atomic orbitals of the X atom are depicted in Figure 2, taking into account that there is the possibility for both linear and C_{2v}-symmetric interactions. Basically, these interactions correspond to: (a) charge transfer from an appropriate orbital (a_1 in C_{2v} symmetry, σ in linear geometry) from the X atom to the LUMO of the C_2 moiety; the atomic orbital should be either the 3s orbital for Na and Mg, or the $3p_z$ orbital for the rest of atoms; (b) back-donation from the HOMO of the C_2 unit to the corresponding 3p atomic orbital; (c) charge transfer from an occupied atomic p orbital (b_2 in C_{2v} symmetry, π in linear geometry) to the C_2 next LUMO, that is the $1\pi_g$ antibonding orbital.

For Na and Mg atoms, with high-lying valence orbitals relative to those of the C_2 unit, the dominant interaction is the

(79) Dewar, M. J. S. *Bull. Soc. Chim. Fr.* **1951**, *18*, C71.
(80) Chatt, J.; Duncanson, L. A. *J. Chem. Soc.* **1953**, *2939*.
(81) Bishop, K. C. *Chem. Rev.* **1976**, *76*, 461.
(82) Cremer, D.; Kraka, E. *J. Am. Chem. Soc.* **1985**, *107*, 3800.
(83) Cremer, D.; Kraka, E. *J. Am. Chem. Soc.* **1985**, *107*, 3811.
(84) Grev, R. S.; Schaefer, H. F. *J. Am. Chem. Soc.* **1987**, *109*, 6577.
(85) Liang, C.; Allen, L. C. *J. Am. Chem. Soc.* **1991**, *113*, 1878.
(86) Byun, Y. G.; Saebo, S.; Pittman, C. U. *J. Am. Chem. Soc.* **1991**, *113*, 3689.

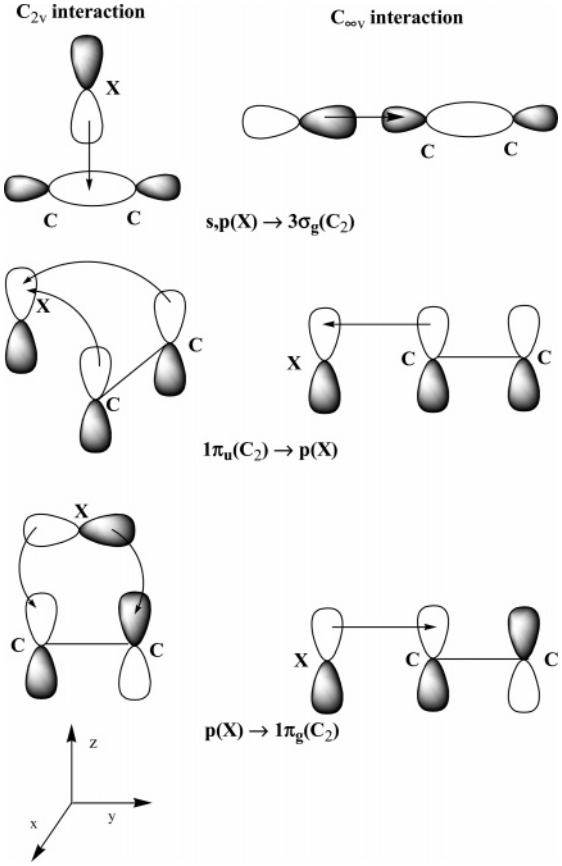

Figure 2. Schematic representation of the main interactions between the valence orbitals of the X and C_2 fragments. The coordinate axes are for the cyclic structures. For linear isomers the *z*-axis corresponds to the molecule axis.

first one, taking place from the 3s orbital, that is a 3s(X) → $3\sigma_g(C_2)$ charge transfer (HOMO → LUMO). Back-donation from C_2 is rather small due to the high energy of the 3p(X) orbitals. In any case the $1\pi_u(C_2) \rightarrow$ 3p(X) interaction for C_{2v} symmetry can take place in this case not only through π overlapping (as represented in Figure 2), but also through σ overlapping due to the vacant $3p_z$(X) orbital (a_1 symmetry) which can interact with the in-plane $1\pi_u(C_2)$ orbital. In both cases therefore accumulation of electron density takes place through the line connecting atom X with the middle point of the C_2 moiety, and therefore T-shape structures should be found for C_{2v} interaction, in agreement with the previous topological analysis of the electronic density. It is also worth pointing out that, since this interaction is more favorable for C_{2v} symmetry than for $C_{\infty v}$ symmetry, the linear isomers are expected to be less stable than the cyclic ones.

For atoms such as Al or Si, charge transfer takes place mainly from the $3p_z$ orbital. This 3p(X) → $3\sigma_g(C_2)$ interaction is still the dominant one, although $1\pi_u(C_2) \rightarrow$ 3p(X) back-donation starts to be significant. As a consequence the main features of the electronic density are similar to the sodium and magnesium compounds (T-shape structures are found in C_{2v} symmetry), but some new features appear. For example $1\pi_u(C_2) \rightarrow$ 3p(X) interaction in these cases is more favorable for linear geometries, because there are two different vacant 3p orbitals of appropriate π symmetry, whereas in the case of C_{2v} symmetry interaction can only take place with the $3p_x$ orbital (b_1 symmetry), because the corresponding a_1 orbital (coming from the $3p_z$ atomic orbital) which could interact with the appropriate π_u orbital (a_1 symmetry) of the C_2 unit is half-occupied in the case of Al and doubly occupied for Si. Therefore, an inversion in the trend observed for the cyclic-linear energy separation (see Table 3) is observed at the B3LYP level (and at the HF level, although the values are not shown in Table 3) for C_2Al.

The higher electronegativity of P, S, and Cl compared with Na, Mg, Al, and Si makes that 3p(X) → $3\sigma_g(C_2)$ charge-transfer play a somewhat smaller role. This is in part compensated by the possibility of 3p(X) → $1\pi_g(C_2)$ interaction, since now the appropriate 3p orbitals (the 3p orbital of b_2 symmetry for cyclic geometries, both π orbitals in $C_{\infty v}$ symmetry) are either partially or completely occupied. Of course $1\pi_u(C_2) \rightarrow$ 3p(X) back-donation is now also more favorable because the energy gap between both sets of orbitals has narrowed as compared with the situation for the more electropositive atoms. Therefore the general view is an enhancement of peripheral X−C bonding in C_{2v} symmetry accompanied by a decreasing electronic density through the line connecting the X atom with the middle point of the C−C bond. This is compatible with the previous observation of truly cyclic structures for C_2P, C_2S, and C_2Cl. Nevertheless the most important feature is that linear structures are favored since again in $C_{\infty v}$ symmetry both 3p orbitals of π symmetry may take part in both interactions. It should be noted that for the 3p(X) → $1\pi_g(C_2)$ interaction in C_{2v} symmetry one of the π_g orbitals is of a_2 symmetry, and therefore no interaction with a 3p orbital can be established.

Of course, we have highlighted the main interactions active in C_2X compounds. Nevertheless there are other interactions that play a somewhat smaller role, but are also worthwhile to mention. For example, the role of d orbitals is obviously more important as one moves from sodium to chlorine. In the case of linear isomers, the d populations of the X atom vary form 0.04 (Na) to 0.12 (Cl). For the cyclic isomers, the lowest d population is also found for sodium (0.04), whereas the highest one is found for sulfur (0.20).

Let us focus now on some of the geometrical parameters. As can be seen in Tables 1 and 2, the C−C carbon distances increase considerably when passing from the more electropositive atoms to the more electronegative ones, and this can be interpreted in terms of the theoretical model. In those cases where there is a low degree of $1\pi_u(C_2) \rightarrow$ 3p(X) back-donation (less electronegative atoms), the C−C bond distances are close to the corresponding C−C bond length in C_2 (1.247 Å and 1.250 Å, respectively, at the B3LYP and QCISD levels), whereas for those elements where this interaction is relatively high (P, S, and Cl) the C−C distance is considerably increased.

Therefore, this simple picture in terms of interactions between the orbitals of both fragments, X and C_2, is in good agreement with the observations about the molecular structure of C_2X compounds. The competition between linear and cyclic arrangements, the formation of truly cyclic isomers or T-shape structures in C_{2v} symmetry, as well as some basic features of the geometrical parameters can be interpreted through this model.

Detailed Analysis of the Variation of Total Energy and Orbital Energies with the Geometry in C_2X Compounds. Despite a simple model might help to understand the basic features of C_2X compounds, it would be interesting to have a detailed knowledge of one of their most important features, that

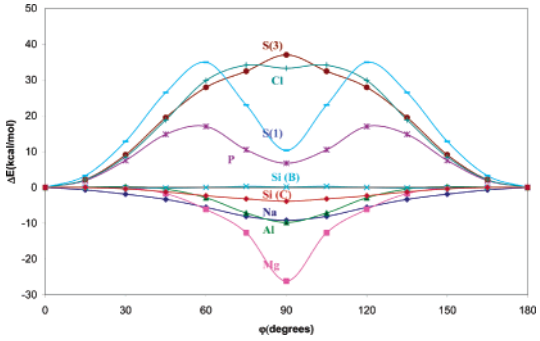

Figure 3. Variation of the total energy (in kcal/mol, relative to the linear geometry), computed at the B3LYP/6-311+G(3df) level, for the different C_2X compounds with the angle (φ) between the line connecting the X atom and the middle point of the C−C bond. The curve denoted Si(B) corresponds to the B3LYP level, whereas Si(C) has been obtained at the CCSD(T)/6-311+G(3df) level on the B3LYP geometries. S(1) and S(3) denote the C_2S singlet and triplet, respectively, curves.

is the competition between linear and cyclic isomers. For that reason, we have analyzed the variation of the total energy and the orbital energies with the geometry.

The total energy as a function of the angle (φ) between the line connecting the X atom with the middle point of the C−C bond for the different C_2X species is shown in Figure 3. In these representations the linear isomer is placed at $\varphi = 0$, whereas the C_{2v}-symmetric structure corresponds to $\varphi = 90$. The curves have been obtained optimizing the C−C and X−(C−C) distances for various fixed φ angles at the B3LYP/6-311+G-(3df) level of theory. In the case of sulfur, we show the curves obtained for the singlet and triplet states, which are denoted as S(1) and S(3), respectively.

It is readily seen that there are basically two different general behaviors. For Na, Mg, and Al systems there is a continuous decreasing energy from the linear isomer to the C_{2v}-symmetric structure, the latter being more stable. This is consistent with the fact that linear isomers have in all these cases an imaginary frequency, and therefore the linear species is just the transition state for the degenerate rearrangement of the T-shape structure. On the other hand for the systems containing P, S, or Cl, the linear isomer is the most stable one. Nevertheless for C_2P and C_2Cl the cyclic species is a true minimum (in agreement with the frequency analysis), and one can identify in Figure 3 the location of the corresponding transition states connecting them with the respective linear isomers. For C_2S, a triplet in its ground state, it can be seen that the energy increases continuously and the cyclic structure is a transition state. However, this should be considered a somewhat anomalous behavior of the triplet state of C_2S. In fact, the curve corresponding to singlet C_2S is qualitatively similar to those of C_2P and C_2Cl. The cyclic isomer is a true minimum on the singlet potential surface, and the energy difference between the linear and cyclic species lies just between the corresponding values for the phosphorus and chlorine compounds.

It is worth noting that C_2Si is a turning point in this behavior. In fact, at the B3LYP level, the Si(B) curve, the surface is so flat that the representation is almost coincident with the abscissas axis (the energy variations are always below 0.3 kcal/mol). The curve denoted Si(C) has been obtained employing the CCSD-(T)/6-311+G(3df) level at the optimized B3LYP geometries. It is now observed in the Si(C) curve that its behavior is similar to that found for its Na, Mg, and Al counterparts, although with

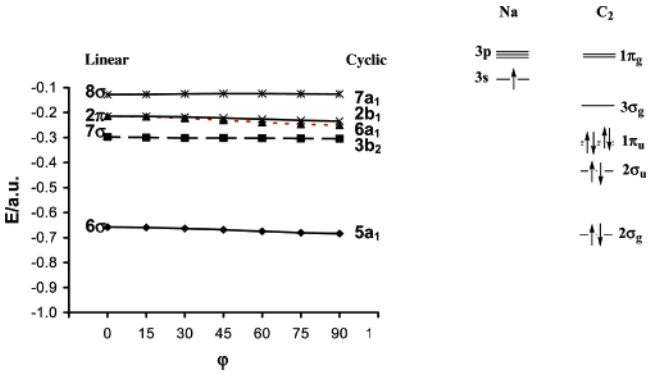

Figure 4. Variation of the molecular orbital energies (a.u.) with the φ angle for the C_2Na system.

a smoother variation in the energy. This result suggests that the linear SiCC species should not be considered as a true minimum, and also confirms the need for high-order ab initio methods for a reliable prediction on C_2Si. It is also interesting to point out that the *polytopism*[23] of C_2Si is not only related to the ionic character of the bonding in this molecule, which can be described as composed of Si^+ and C_2^- fragments. The polytopic character of a molecule was first introduced by Clementi et al.[87] when studying the extremely flat potential surface found in lithium cyanide for the pinwheel motion of Li^+ around CN^-. C_2Na, C_2Mg, and C_2Al can be described in a similar way as X^+ bonded to a C_2^- moiety, but only in the case of C_2Si the flatness is so extreme. It seems that this is due to the limiting character of silicon, since the ionic character of the bonding tends to favor the cyclic species but also covalent interactions begin to be important. The balance of both trends results in a very flat surface. It is worth noting that the Si_2C system has a similar behavior to C_2Si.[88]

To gain more insight into the bonding in these compounds, we have analyzed the evolution of the molecular orbitals when passing from the linear to the cyclic arrangements. We show in Figures 4, 5, and 6 three representative cases of the different types of behaviors that we have observed, corresponding to different relative dispositions of the atomic valence orbitals and the molecular orbitals of the C_2 unit: C_2Na, C_2Si, and triplet C_2S. Na has atomic 3s and 3p orbitals lying much higher than the molecular orbitals of the C_2 unit. Therefore, the interactions between the orbitals of both fragments are rather small, and so are the differences in orbital energies between the linear and C_{2v}-symmetric arrangements. Nevertheless it can be seen in Figure 4 that the 6σ-$5a_1$ orbital is slightly more stable for the cyclic isomer, as a consequence of the higher overlap between the s and p_z orbitals with the C_2 $3\sigma_g$ orbital following a C_{2v} approach compared with the overlap in a linear approach. Of course the energy difference between the interacting orbitals is very high and the stabilization is very small. A similar situation is observed for the interaction between the $3p_z$ and $3p_x$ orbitals with the $1\pi_u$ set of molecular orbitals. The interaction is also rather small, and is somewhat more favorable for the cyclic arrangement. Consequently, the energies of the $6a_1$ and $2b_1$ orbitals are slightly more favorable than their 2π counterparts. On the other hand, the energy of the 7σ-$3b_2$ orbital varies only slightly with the φ angle. Most of the charge transfer in this

(87) Clementi, E.; Kistenmacher, H.; Popkie, H. *J. Chem. Phys.* **1973**, *58*, 2460.
(88) Torrent-Sucarrat, M.; Luis, J. M.; Duran, M.; Sola, M. *J. Chem. Phys.* **2004**, *120*, 10914.

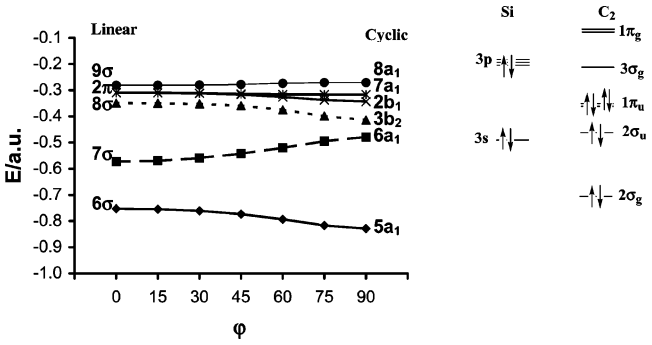

Figure 5. Variation of the molecular orbital energies (a.u.) with the φ angle for the C_2Si system.

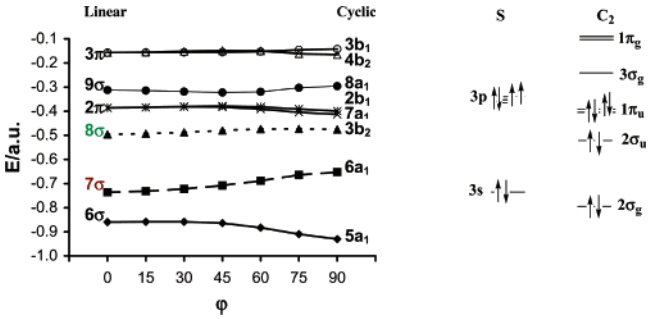

Figure 6. Variation of the molecular orbital energies (a.u.) with the φ angle for the C_2S system.

compound comes from the interaction between the Na 3s orbital (singly occupied) and the C_2 $3\sigma_g$ orbital (LUMO). This is the strongest interaction in principle, since the energy difference between them is smaller than in the other cases. This interaction is only slightly more favorable for the linear arrangement, and therefore the 8σ-$7a_1$ orbital increases only slightly its energy when passing from the linear to the C_{2v}-symmetric geometry. The overall balance from Figure 4 is that the cyclic (in fact T-shape) isomer is favored.

For silicon dicarbide (Figure 5) the stabilization of the $5a_1$ molecular orbital is higher than in the case of C_2Na, because the 3s orbital of silicon is closer in energy to the C_2 $2\sigma_g$ orbital. Nevertheless, the main difference with the sodium dicarbide is that the silicon 3s orbital now lies very close to the $2\sigma_u$ orbital of C_2, and therefore in linear geometry they may combine to form two molecular orbitals (7σ and 8σ). On the other hand, in C_{2v}-symmetry the silicon 3s orbital (a_1 symmetry) cannot interact with the $2\sigma_u$ orbital of C_2 (b_2 symmetry), and combines with one of the $1\pi_u$ orbitals. The result is obviously that 7σ is more stable than $6a_1$, but 8σ is less stable than its $3b_2$ counterpart (which remains virtually at an energy quite close to that of the $2\sigma_u$ orbital). For C_2Si again the interaction between the $3p_z$ and $3p_x$ orbitals with the $1\pi_u$ set of molecular orbitals slightly favors the cyclic arrangement. Finally, as in the case of C_2Na, there is also a large amount of charge transfer from silicon toward the C_2 moiety through the interaction of the $3p_z$ orbital with the $3\sigma_g$ orbital (in the schematic representation we have considered that C_2Si correlates with $Si(^1S) + C_2(^1\Sigma_g^+)$, but a similar conclusion is reached considering triplet silicon and triplet C_2). Again this interaction is only slightly more favorable for the linear arrangement. The overall result for C_2Si is that, due to the opposite variations with the φ angle of the orbital energies, the cyclic arrangement seems to be only slightly favored.

In the case of C_2S (Figure 6) the interaction between the atomic 3s orbital and the C_2 $2\sigma_g$ orbital is stronger, since they lie relatively close in energy, and they combine to form the $5a_1$ and $6a_1$ orbitals in C_{2v} symmetry (6σ and 7σ for linear geometry). Since this is a four-electron interaction the result is destabilizing. The overlap is higher for cyclic geometries and therefore the 6σ-$5a_1$ orbital lowers its energy with increasing φ angle, whereas for the 7σ-$6a_1$ orbital the trend is obviously the opposite. In summary this interaction favors the linear geometry. The sulfur $3p_y$ orbital and the C_2 $2\sigma_u$ are also not too far in energy and may combine to give a $3b_2$ orbital. Since the overlap between these two orbitals is more favorable in linear geometries, the result is that the $3b_2$ orbital increases its energy with the φ angle. As for the other dicarbides, again the interaction between the $3p_z$ and $3p_x$ orbitals with the $1\pi_u$ set of molecular orbitals slightly favors the cyclic arrangement. The 9σ-$8a_1$ molecular orbital comes from the occupation of the C_2 $3\sigma_g$ orbital, which is stabilized through interaction with the corresponding sulfur 3p orbital. Again this interaction is more favorable for the linear geometry and therefore the energy is higher for the cyclic arrangement. Incidentally, it should be stressed that occupation of this orbital implies a certain amount of charge transfer from sulfur toward the C_2 unit. The singly occupied $3b_1$ orbital (resulting from the $3p_x$-$1\pi_u$ antibonding combination) follows the opposite pattern than its $2b_1$ counterpart, and slightly favors the cyclic geometry. Finally, the second singly occupied $4b_2$ orbital (essentially of $3p_y$-$2\sigma_u$ antibonding character) is slightly more favorable for the cyclic geometry, that is just the opposite behavior to its bonding partner $3b_2$. The overall balance is that the linear geometry has lower molecular orbital energies in this case.

Of course, the preceding discussion only refers to the molecular orbital energies. There are other factors that should be taken into account in order to obtain a conclusion about the preferred arrangement for C_2X compounds. One of the most important is of course the electron correlation energy. We have computed the correlation energy as the difference between the CCSD(T)/6-311+G(3df) and the HF/6-311+G(3df) electronic energies. The differences between the correlation energies of the linear and cyclic C_2X species are given in Table 3 (a positive value means that the correlation energy is higher for the cyclic isomer). It is usually assumed that electron correlation tends to favor cyclic isomers over open-chain ones. The results provided in Table 3 show that this is certainly right for truly cyclic species, such as C_2P, C_2S, or C_2Cl, but not necessarily for T-shape compounds. In the cases of C_2Na and C_2Si electron correlation favors the C_{2v}-symmetric species, but for C_2Mg and C_2Al the linear isomer is favored. This is particularly evident for C_2Mg.

Finally, it would be convenient to have some knowledge about the stability of the different second-row dicarbides. The dissociation energies for C_2X compounds are shown in Table 6. Dissociation energies have been computed for the $C_2X \rightarrow X + C_2$ process at the CCSD(T) level including ZPVE corrections. For C_2Si, C_2P, and singlet C_2S, we have considered the dissociation into the corresponding ground state of the X atom (^3P, ^4S, and ^3P, respectively, for Si, P, and S) and the lowest-lying triplet state ($^3\Pi_u$) of the C_2 unit. In all other cases, the dissociation process leads to the singlet ground state of C_2. The general trend observed in Table 6 is that the dissociation energies increase from both extreme atoms (Na and Cl), to the center of the second-row (Si), where the different interactions between

Table 6. Dissociation Energies (in kcal/mol) for the $C_2X \rightarrow X + C_2$ Processes at the CCSD(T) Level of Theory Including ZPVE Corrections[a]

	isomer	
C_2X	linear	cyclic
C_2Na	79.11	88.55
C_2Mg	69.34	81.37
C_2Al	101.11	116.09
C_2Si	144.08	147.88
C_2P	112.29	108.92
$C_2S(1)$[b]	106.66	100.92
$C_2S(3)$[c]	118.68	87.18
C_2Cl	85.56	55.24

[a] The calculations have been made considering the lowest-lying electronic state of the X atom and the corresponding C_2 state of the correct spin multiplicity ($^3\Pi_u$ for C_2Si, C_2P, and Singlet C_2S; $^1\Sigma_g$ for the rest of systems). [b] Singlet state. [c] Triplet state.

the valence orbitals of the heteroatom and C_2 are relevant. In any case, it can be seen in Table 6 that all C_2X ground states (cyclic for C_2Na, C_2Mg, C_2Al, and C_2Si; linear for C_2P, C_2S, and C_2Cl) have relatively high dissociation energies, the smallest one being 85.56 kcal/mol for linear C_2Cl. The largest dissociation energy (147.88 kcal/mol) is found for cyclic C_2Si, a value which is not far from previous estimates, bearing in mind the intrinsic difficulties for estimating the energetics of C_2Si through theoretical calculations.[23] Nielsen et al.[23] obtained a theoretical prediction of 151.42 kcal/mol for the same dissociation process.

Conclusions

The molecular structure of the second-row dicarbides C_2X (X = Na−Cl) has been theoretically studied. Special attention has been paid to the competition between linear and cyclic isomers. In agreement with previous studies it is found that C_2Na, C_2Mg, and C_2Al clearly preferred a C_{2v}-symmetric arrangement, whereas for C_2P, C_2S, and C_2Cl the linear isomer is predicted to be the ground state. C_2Si represents a limiting case, and the C_{2v}-symmetric isomer is found to lie just about 3.8 kcal/mol below the linear isomer at the most reliable level of theory employed. A topological analysis of the electronic density has revealed that for C_2Na, C_2Mg, C_2Al, and C_2Si the C_{2v}-symmetric isomer corresponds in fact to a T-shape structure, whereas for C_2P, C_2S, and C_2Cl it is a truly cyclic structure with peripheral X−C bonds. The main features of these compounds have been rationalized in terms of a simple model that incorporates the most relevant interactions between the valence orbitals of both fragments, the X atom and the C_2 molecule. A detailed analysis of the variations of both total energies and orbital energies for second-row dicarbides with the angle between X and the middle point of the C−C bond has been carried out. This study allows a deeper knowledge of the factors governing the linear-cyclic competition in these compounds. It is hoped that this study could help understanding the behavior of other small heteroatom-doped carbon clusters.

Acknowledgment. This research has been supported by the Ministerio de Ciencia y Tecnología of Spain (Grant BQU2001-3660-C02-02) and by the Junta de Castilla y León (Grant VA085/03).

JA046017P